buildings

MDPI

Article

Cement-Free Geopolymer Paste: An Eco-Friendly Adhesive Agent for Concrete and Masonry Repairs

Tayseer Z. Batran, Mohamed K. Ismail *, Mohamed I. Serag and Ahmed M. Ragab

Department of Structural Engineering, Faculty of Engineering, Cairo University, Giza 12613, Egypt
* Correspondence: mkismail@eng.cu.edu.eg; Tel.: +20-1002718-100

Abstract: This study aimed to investigate the feasibility of using geopolymer paste (GP) as an adhesive agent for (i) anchoring steel bars in concrete substrates, (ii) repairing concrete, and (iii) repairing limestone and granite masonry blocks commonly found in historic buildings. In this investigation, seven cement-free GP mixes were developed with different combinations of binder materials (slag, silica fume, and metakaolin). The mechanical properties, adhesive performance, and production cost of the developed GP mixes were compared to those of a commercially epoxy adhesive mortar (EAM). The results obtained from this study indicated that the use of GPs enhanced the bonding between steel bars and concrete substrates, achieving bonding strengths that were 19.7% to 49.2% higher than those of control specimens with steel bars directly installed during casting. In concrete repairs, the GPs were able to restore about 60.6% to 87.9% of the original capacity of the control beams. Furthermore, GPs exhibited a promising performance in repairing limestone and granite masonry blocks, highlighting their potential suitability for masonry structures. The best adhesive performance was observed when a ternary binder material system consisting of 70% slag, 20% metakaolin and 10% silica fume was used. This combination, compared to the investigated EAM, showed comparable adhesive properties at a significantly low cost, indicating the viability of GPs as a cost-effective, eco-friendly adhesive agent.

Keywords: adhesive performance; geopolymer paste; metakaolin; slag; silica fume; concrete; masonry; repair applications

check for updates

Citation: Batran, T.Z.; Ismail, M.K.; Serag, M.I.; Ragab, A.M. Cement-Free Geopolymer Paste: An Eco-Friendly Adhesive Agent for Concrete and Masonry Repairs. *Buildings* **2024**, *14*, 3426. https://doi.org/10.3390/buildings14113426

Academic Editor: Hailong Ye

Received: 26 September 2024
Revised: 17 October 2024
Accepted: 25 October 2024
Published: 28 October 2024

Copyright: © 2024 by the authors. Licensee MDPI, Basel, Switzerland. This article is an open access article distributed under the terms and conditions of the Creative Commons Attribution (CC BY) license (https://creativecommons.org/licenses/by/4.0/).

1. Introduction

Structures may suffer many serious damages during their service life due to overloading and/or harsh environmental attacks [1]. This can result in significant local damages such as cracking, spalling, material deterioration and reinforcing rebar corrosion [2,3]. Such damage may, under severe conditions, compromise the integrity and stability of the structure, potentially leading to total collapse. Therefore, repairing the induced damage is essential for extending the service life of structures and maintaining their design capacity. Repairs can be carried out using various approaches, including (i) filling cracks and cavities, (ii) replacing damaged material with either a new layer of the same type or a higher-performance material, and (iii) installing additional reinforcing steel bars. However, for the repair to be effective, it is crucial to achieve strong bonding at the interface (i.e., the weakest zone) between the existing material and the new one. The bonding strength at this interface is influenced by several factors. For instance, the mechanical properties of both the repair and substrate materials affect their bonding; greater compatibility between these properties generally leads to stronger bonding [4,5]. Increased roughness of the substrate surface also improves bonding with the new material [6,7]. Additionally, applying an adhesive agent at the interface can significantly enhance the interfacial bonding between layers [5,8,9]. Thus, adhesive agents are often a valuable option for various repair tasks.

For various repair applications, many commercial adhesives are available, which are generally classified into organic-based and inorganic-based types [10–12]. Organic

adhesives, such as epoxy resin, are often quite expensive [13]. On the other hand, inorganic-based adhesives, especially those that are cement-based, are not environmentally friendly due to their inclusion of cement [9]. The production of cement consumes natural resources and generates substantial CO_2 emissions, contributing approximately 7% of the total global CO_2 emissions [14]. Additionally, the energy required for cement production accounts for approximately 12–15% of total industrial energy use [15–17]. Consequently, there is a growing demand for alternative adhesives that are both cost-effective and environmentally friendly. Recently, there has been increasing interest in alkali-activated binders, or geopolymer binders, as innovative construction materials that offer lower costs and reduced environmental impacts. Geopolymers are typically produced through the alkaline activation of materials rich in silica and alumina, such as metakaolin (MK), fly ash (FA), slag (SL), and silica fume (SF) [4,17]. Compared to cement, MK is produced at a lower cost, with reduced energy consumption and significantly lower CO_2 emissions [4,18]. Other binders like FA, SL, and SF are industrial by-products that are recycled without generating additional CO_2 emissions [4], thereby mitigating environmental issues and conserving natural resources [4,17,18].

Reviewing the existing literature, several studies have investigated the performance of two-layer systems composed of a geopolymer layer (including concrete, mortar, and paste) and a conventional concrete layer. These studies employed various tests, such as slant shear, bi-surface shear, splitting tensile, pull-off, and direct tension tests [6,12,13,19–23]. The results demonstrated high bonding strength between the repair geopolymer layer and the concrete substrate layer, highlighting the potential of geopolymers as an effective repair material. Other limited studies have focused on using geopolymer paste (GP) or geopolymer mortar (GM) as adhesive agents to strengthen concrete or anchor steel rebars in concrete substrates. For example, Ding et al. [24] used an SL/FA-based GP to fill fractures in concrete prism substrates. They varied the alkali activator with three different molar ratios while keeping the binder composition constant at 30% FA and 70% SL. The repaired prisms were tested for compression and flexural strength, demonstrating repair efficiencies of up to 120% and 116%, respectively. Songpiriyakij et al. [9] investigated the bonding performance of an FA-based GP modified with rice husk, bark ash, and SF for anchoring steel rebar in concrete substrates. They found that incorporating SF with FA allowed the GP to effectively bond rebar to the concrete substrate. The mechanical and bonding characteristics of FA-based GP were also assessed by Zailani et al. [25] when varying NaOH concentrations (8, 10, 12, and 14 M) were used, determining that 12 M was the optimal concentration. Frangieh et al. [26] examined the performance of an MK-based GP for binding cracked concrete. The repaired specimens were tested under compression and compared to undamaged specimens cast with normal concrete, showing promising results for GP in repairing damaged concrete. Chen et al. [27] also proposed MK-based GM modified with SL, which demonstrated good performance for pavement repairs. Furthermore, Maras [28] introduced GM made of lime, brick powder, and SL for the repair of heritage masonry buildings. Hai et al. [29] employed thermal-activated red mud along with SL to produce geopolymer repair mortar. Zheng et al. [30] utilized SL and waste glass fiber-reinforced polymer powder in developing GMs with a short setting time, high flowability, excellent early mechanical strength and bond properties, indicating its potential for use as a rapid repair material for concrete or as a protective coating in corrosive environments.

Contributing to further evaluating the feasibility of using geopolymer products for repair applications, this study aimed to investigate SL-based GP modified with SF and/or MK as an adhesive agent, with the goal of defining an optimal binder system. In total, seven cement-free GP mixes were developed using various unary, binary and ternary combinations of SL, SF and/or MK. The developed GP mixes were first evaluated using slump, compressive strength, and splitting tensile strength (STS) tests. Then, the adhesive performance of these GPs was assessed in several applications: anchoring steel rebar in concrete substrate, and filling fractures in concrete and masonry blocks (limestone and

granite commonly found in historic buildings). A commercial epoxy adhesive mortar (EAM) was also included in the study for comparison. Finally, the outcomes of this investigation can help clarify the potential of using GP as an eco-friendly and cost-effective alternative to high-cost commercial adhesive agents.

2. Experimental Program

2.1. Material Properties and Mix Proportions

The materials used in this study were detailed as follows:

- The GP mixes were developed using different binder materials, namely SL, SF and MK, similarly to ASTM C989 [31], ASTM C1240 [32] and ASTM C618 (Class N) [33], respectively. The chemical and physical properties of the binder materials are shown in Table 1. Sodium silicate solution (Na_2SiO_3. H_2O) and sodium hydroxide (NaOH) flakes with 98% purity and specific gravity of 1.53 and 2.13, respectively, were used as the alkaline activator. A polycarboxylate-based high-range water-reducer admixture (HRWRA) similarly to ASTM C494 [34] was used to adjust the workability of the developed GP mixes. Table 2 shows the mixture compositions of the developed GP mixes.
- A commercially available epoxy adhesive mortar (EAM) (complies with ASTM C 881 [35]) was used as a bonding agent for comparison. The compressive strength, flexural strength, and adhesive strength of the EAM were 80 MPa, 40 MPa and 10.3 MPa, respectively.
- Concrete substrate was developed with 350 kg/m^3 ordinary Portland cement Type I (ASTM C150 [36]) as the binder material and a water-to-binder ratio of 0.4. Crushed dolomite aggregates with a maximum size of 12 mm and specific gravity of 2.73 were used as a coarse aggregate, while the fine aggregate was natural sand with a maximum aggregate size of 4.75 mm and specific gravity of 2.5. The concrete substrate was designed and cast to achieve a 28-day compressive strength of 30 MPa. This mix was used to cast prisms for pull-out and flexural tests.
- Granite and limestone blocks typically found in several historic buildings, were used in this study in order to investigate the adhesive performance of GP mixes in repairing damaged masonry structures.
- Steel rebar: deformed steel reinforcing bars with a diameter of 16 mm, average yield stress of 417 MPa and average ultimate tensile stress of 725 MPa, were used in steel-concrete pull-out tests.

Table 1. Chemical and physical properties of binder materials used.

Chemical Properties (%)	Cement	SL	SF	MK
SiO_2	20.1	35.4	92	54.5
Al_2O_3	5.32	17.4	1.1	37.5
Fe_2O_3	3.61	1.40	1.45	1.25
CaO	61.7	36.87	1.2	0.09
MgO	2.48	6.83	1.55	0.04
Na_2O	0.37	-	-	<0.05
K_2O	0.13	0.37	1.45	<0.40
L.O.I	2.05	1.0	0.57	0.95
Physical properties				
Specific gravity	3.15	2.9	2.2	2.56
Blaine fineness (m^2/kg)	410	408	20,000	1390

Table 2. Composition of GP mixes.

Mix #	Mixture	SL/BC	SF/BC	MK/BC	W/BC	Na_2SiO_3/BC	NaOH/BC	HRWRA/BC%
M1	100SL	1	-	-	0.4	0.3	0.1	0.67
M2	90SL +10SF	0.9	0.1	-	0.4	0.3	0.1	0.76
M3	80SL + 20SF	0.8	0.2	-	0.4	0.3	0.1	0.82
M4	70SL + 30SF	0.7	0.3	-	0.4	0.3	0.1	0.92
M5	90SL + 10MK	0.9	-	0.1	0.4	0.3	0.1	1.01
M6	80SL + 20MK	0.8	-	0.2	0.4	0.3	0.1	1.27
M7	70SL + 10SF + 20MK	0.7	0.1	0.2	0.4	0.3	0.1	1.54

Note: BC = binder content; SL = slag; SF = silica fume; MK = metakaolin; W/BC = water-to-binder content; Na_2SiO_3 = sodium silicate; NaOH = sodium hydroxide; HRWRA = high-range water-reducer admixture.

2.2. Details of GP Mixes and Mixing Procedures

In this study, seven cement-free GP mixes were developed with unary, binary, and ternary binder materials (see Table 2), detailed as follows:

- The first mix (M1) was developed using 100% SL as the binder material and did not include any cement.
- The second, third, and fourth mixes (M2, M3, and M4) were produced similarly to M1, but the SL was partially replaced by SF at percentages of 10%, 20%, and 30%, respectively.
- The fifth and sixth mixes (M5-M6) were developed similarly to M1, but the SL was partially replaced by MK at percentages of 10% and 20%, respectively.
- The seventh mix (M7) was developed with a ternary binder material system consisting of 70% SL + 20% MK + 10% SF. This mix was designed to incorporate the optimal replacement levels of SF and MK based on the results obtained from M1 to M6.

For all mixes, the alkali activator solution was a mixture of sodium silicate (Na_2SiO_3) and sodium hydroxide (NaOH) solutions (the Na_2SiO_3 to NaOH mass ratio was kept at 3.0). Since the NaOH was in a solid flake form, the distilled water was mixed with NaOH flakes to prepare a solution with a molarity of 14M. Then, the solution was left to cool down to around 30 °C. It should be noted that the Na_2SiO_3 to NaOH mass ratio and the molarity of NaOH solution, were chosen based on a trial mixes stage conducted by authors to achieve the maximum compressive strength. These values are in agreement with what has been recommended by other researchers [11,37,38].

The preparation of the GP mixes began with a 2-min dry mixing of the binder materials (if more than one cementitious material was used). Next, the sodium silicate and sodium hydroxide solutions were mixed together and added to the blended binder materials. During mixing, the HRWRA was used to adjust the workability of each mix to achieve the target slump flow of 220 ± 20 mm diameter.

2.3. Specimen Design, Preparation, Curing and Testing

2.3.1. Fresh and Mechanical Properties

The flowability of the developed mixes was evaluated using the mini-slump test following the procedure given in EFNARC [39]. The compressive strength test was conducted on 50 mm cubic specimens (as per ASTM C109 [40]), while the splitting tensile strength (STS) test was carried out using 10 mm diameter × 50 mm high cylinders.

2.3.2. Specimens and Procedures of Pull-Out Test

To evaluate the adhesive performance of GP mixes for anchoring steel rebar in a concrete substrate, prisms with a size of 150 mm × 150 mm × 200 mm were cast. Prior to casting, a plastic tube with a 20 mm diameter was fixed at the center of each prism. After 24 h, the formworks were demolded, and the plastic tubes were removed. Then, all specimens were moist-cured for 28 days. After curing, the holes were cleaned and the adhesive (i.e., GP mixes) was used to fill more than 50% of their volume. Then, steel

bars with a 16 mm diameter were vertically embedded. It should be noted that the steel bars were also coated with the adhesive before being inserted into the hole in order to ensure that the gap between the steel rebar and the concrete substrate was fully filled. All specimens underwent a pull-out test 28 days after the date of anchoring the bars in concrete. The pull-out strengths of the specimens bonded with GP mixes were compared to those of the control specimens that had steel bars embedded during casting. The specimens' geometry, details, and test setup are shown in Figure 1.

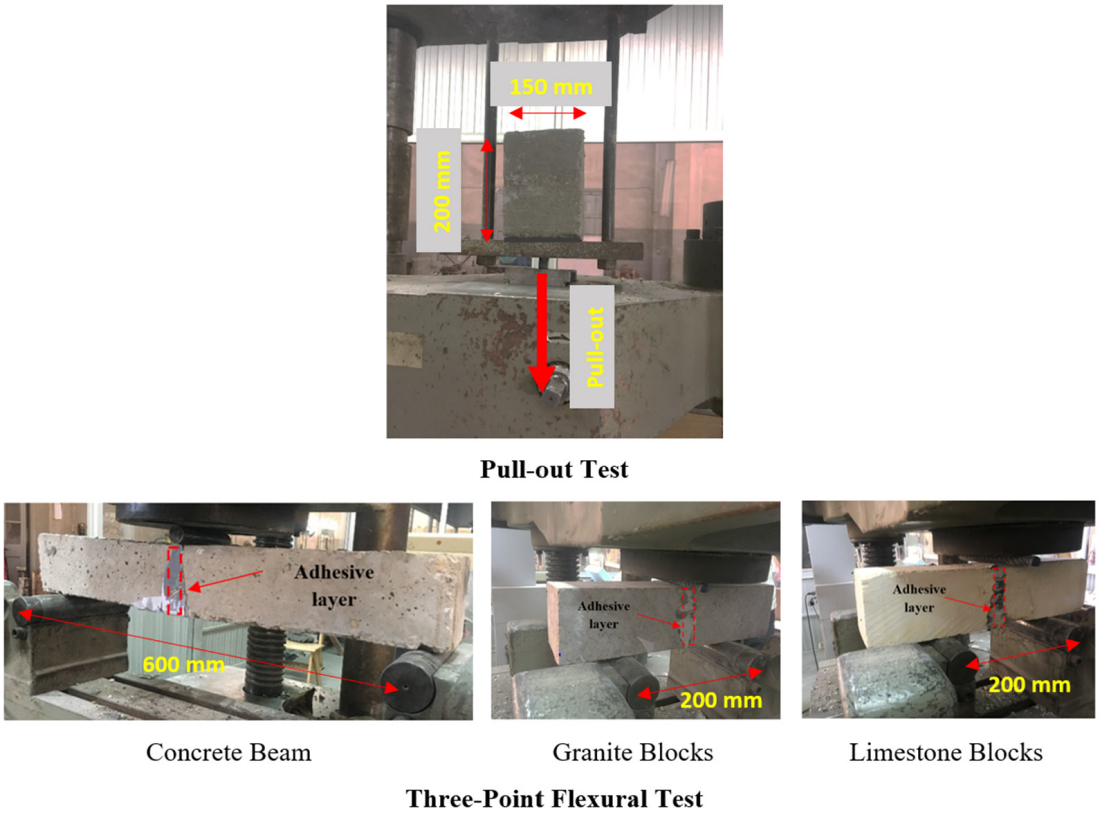


Figure 1. Test setup and specimens' geometry.

2.3.3. Specimens and Procedures for Repairing Concrete

Small-scale beams of 100 mm × 100 mm × 700 mm were cast using the normal concrete mix. Twenty-eight days after casting, the specimens were broken near their midspan using a three-point flexural loading test. After testing, the fracture surface was cleaned to remove any impurities or debris, and thereafter, a layer of GP was applied to bond the two parts of the broken beams. The repaired specimens were covered with a plastic sheet for curing at ambient temperature. After 28 days, the repaired specimens were subjected to a three-point flexural test to assess the restored capacity from the repair in comparison to their original strength. The geometric details of the specimens and the test setup are shown in Figure 1.

It should be noted that inducing cracks in a plain concrete beam proved challenging, as the occurrence of the first crack often led to sudden failure. However, evaluating the restoration of the beam's capacity using GP as an adhesive agent can demonstrate its potential for repairing existing concrete elements with severe cracks.

2.3.4. Specimens and Procedures for Repairing Granite and Limestone Blocks

Granite and limestone blocks (typically found in historic buildings) with a width of 100 mm, a height of 100 mm and a length of 200 mm were used. For each stone type, two blocks were bonded face-to-face using the developed GPs. The bonded specimens were subjected to a three-point flexural test after 28 days of curing, following the same

procedures used for the repaired concrete beams. Details of the specimens and test setup are shown in Figure 1.

It is worth noting that the results of GP mixes obtained from the pull-out and flexural tests were compared with those of the commercially available EAM.

3. Results and Discussion

3.1. HRWRA Demand

The HRWRA-to-binder content (HRWRA/BC) ratios for all developed GP mixes are presented in Table 2. As can be seen, the GP mix developed with only SL (M1) reached the target flowability (slump diameter of 220 ± 20 mm) at a HRWRA/BC ratio of 0.67. The ratio was obviously increased when the SF was added. This could be attributed to the much higher specific surface area and fineness of SF compared to SL, which in turn negatively affected the workability of paste and required a higher HRWRA demand to maintain the desirable fluidity. With the addition of 10%, 20%, and 30% SF (M2-M4), the HRWRA/BC ratio increased by 13.4%, 22.4%, and 37.3%, respectively, compared to M1. A more pronounced increase in the HRWRA/BC ratio was observed when the SL was replaced by the MK due to the clay nature and the higher specific surface area of MK [41,42]. At 10% and 20% MK replacement levels (M5-M6), the HRWRA/BC ratio increased by 50.7% and 89.6%, respectively, compared to M1, which contains only SL. It is important to note that incorporating a higher dosage of MK was not feasible, as exceeding a 20% replacement level led to a significant increase in HRWRA demand. This, in turn, resulted in a high risk of segregation, excessive retardation, and ultimately a reduction in strength. Similar workability reductions and high HRWRA demands were reported by other researchers when SF and/or MK were introduced into concrete or cement-based mortar [41–44]. Mix M7, which incorporates the optimal percentages of SF and MK (10% and 20%, respectively), achieved the highest HRWRA/BC ratio, which was 2.3 times greater than that required for the SL mix (M1).

3.2. Compressive Strength and STS

Figure 2 and Table 3 show the compressive strength and STS of the developed GP mixes. From the figure, the SL mix (M1) showed a compressive strength and STS of 33.4 MPa and 2.29 MPa, respectively. Strengths were generally improved when the SF was combined with the SL. Among the replacement levels of SF, the use of 10% SF (M2) exhibited the highest improvement in compressive strength and STS, reaching an increase of 25.5% and 12.2%, respectively, compared to the SL mix (M1). Further increasing the SF content beyond 10% (as in M3-M4) resulted in fewer improvements in both compressive strength and STS. Combining SL with MK also resulted in enhancing the compressive strength and STS of GP. The inclusion of 10% and 20% MK (M5 and M6, respectively) led to increasing the compressive strength by 14.1% and 36.3%, respectively, and the STS by 10% and 15.3%, respectively, compared to the SL mix (M1). Replacing the SL with the optimal percentages of both SF and MK (10% and 20%, respectively, as determined from M2 and M6) resulted in the highest increases in compressive strength and STS, with improvements of approximately 42.8% and 24.5%, respectively, compared to the SL mix (M1).

The improvement in the mechanical properties due to the inclusion of SF and/or MK was attributed to their higher silica (Si) and/or alumina (Al) contents (compared to the SL), which dissolve in the alkaline solution and accelerate the polymerization process [45,46]. In addition, the much finer particle size of SF and MK (compared to the replaced SL, as shown in Table 1) improves their filling effect, which in turn yields a better microstructure, i.e., less porosity and denser microstructure. However, as seen in the results, increasing the SF higher than 10% did not show further improvements in the strengths. This result could be attributed to the high SiO_2 content in SF, as shown in Table 1. Consequently, excessive amounts of SF lead to a high Si/Al ratio, which results in a less effective geopolymerization process [47]. Previous studies have also reported contradictory effects of SF. For instance, Alanazi et al. [44] found that introducing SF at any dosage decreased the compressive

strength of FA-based GP. Another study focusing on fly ash/SL blended geopolymer mortar reported that SF had an optimal effect on enhancing mechanical properties at a replacement level of 4% of the total binder content [47]. In contrast, Songpiriyakij et al. [9] found that the maximum compressive strength in FA-based GP was achieved when 40% of FA was replaced with SF. Unlike SF, MK is rich in both silica and alumina. Therefore, even higher MK substitutions were expected to maintain a suitable Si/Al ratio for the polymerization process and yield higher compressive strength [46].

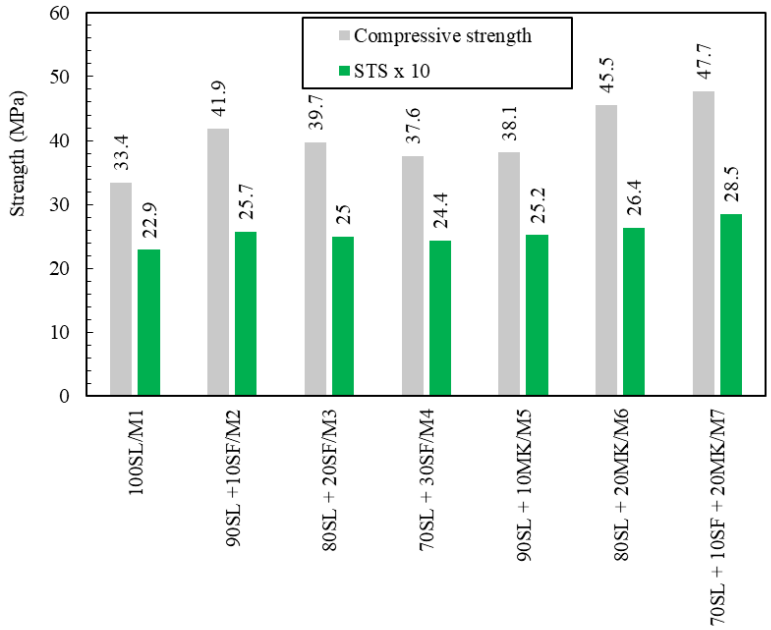


Figure 2. Compressive strength and STS of all developed GP mixes.

Table 3. Testing results.

Mixture	Compressive Strength (MPa)	STS (MPa)	Pull-Out Strength (MPa)	Concrete Beams		Granite Blocks		Limestone Blocks	
				P (kN)	*FM*	*P* (kN)	*FM*	*P* (kN)	*FM*
100SL	33.4	2.29	7.3	2.06	C-GP	7.6	I	8.2	GP-B
90SL + 10SF	41.9	2.57	8.6	2.56	C	9.4	I	10.6	B
80SL + 20SF	39.7	2.50	8.1	2.44	C	9.2	I	10.2	B
70SL + 30SF	37.6	2.44	8.0	2.25	C-GP	8.6	I	10.5	B
90SL + 10MK	38.1	2.52	8.2	2.33	C-GP	8.2	I	9.3	B-I
80SL + 20MK	45.5	2.64	8.8	2.56	C	9.2	I	10.0	B
70SL + 10SF + 20MK	47.7	2.85	9.1	2.99	C	10.2	I	11.0	B

Note: *P* = capacity, *FM* = failure mode; C = failure occurred in concrete; GP = failure occurred in geopolymer layer; I = failure occurred in interface, B = failure occurred in block.

3.3. Pull-Out Strength

Figure 3 and Table 3 exhibit the average pull-out strength of all tested specimens. It can be observed that the pull-out strength of the control specimens (those with a steel bar embedded during casting) was 6.1 MPa. Using the GP mixes developed in this study as an adhesive agent at the concrete–steel interface obviously increased the load required to pull out the steel bar from the concrete substrates. Among the investigated GPs, the mix produced with only SL (M1) showed the lowest pull-out strength with a value of 7.3 MPa, which is 19.7% higher than that of the control specimens. Replacing SL with SF yielded higher strengths, showing the maximum value at a replacement level of 10%. The mix with 90% SL and 10% SF (M2) exhibited a pull-out strength of 8.6 MPa, which is 41%

higher than that of the control specimens. Increasing the addition of SF by higher than 10% showed less improvements. The improved bonding resulting from the use of SF was also confirmed by Songpiriyakij et al. [9], who studied the incorporation of SF into FA-based GP. The pull-out strength of mixes M3 and M4 (with 20% and 30% SF, respectively) were 8.1 and 8.0 MPa, respectively, which was about 32.8% to 31.1% higher than that of the control specimens. For the mixes with 10% and 20% of MK (M5-M6), the pull-out strength was 8.2 MPa and 8.8 MPa, respectively, which were 34.4% and 44.3%, respectively, higher than those of the control specimens. The highest pull-out strength was achieved with the mix containing 70% SL, 20% MK, and 10% SF, reaching 9.1 MPa, which was 49.2% higher than the control specimens. The improvements observed with the addition of SF and/or MK can be attributed to the same factors that contributed to enhancing the compressive strength and STS.

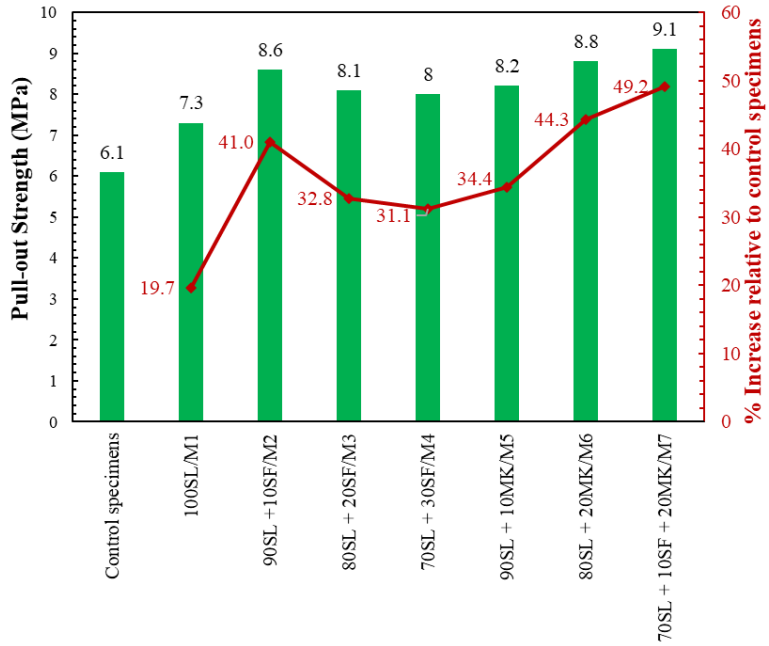


Figure 3. Pull-out strengths.

3.4. Using GP Mixes for Repairing Concrete

Figure 4 and Table 3 show the ultimate loads sustained by all unrepaired and repaired concrete beams. The control beams (unrepaired) sustained an average ultimate load of 3.40 kN. Using the SL mix (M1) for repairing beams, retrieved around 60.6% of the original capacity of the control beams, in which the beams repaired with SL mix exhibited an ultimate capacity of 2.06 kN. Better performance was observed when SF and/or MK were combined with SL. Beams repaired with mixes containing SL and SF (M2–M4) failed after reaching ultimate capacities in a range of 2.25~2.56 kN, which represented around 66.2~75.3% of the flexural capacity of control beams. Consistent with previous results, the M2, M3, and M4 mixes showed that a 10% SF replacement level achieved the maximum capacity restoration. Similar improved results were observed when GP mixes with SL and MK were used for repair. The ultimate capacities achieved were 68.5% and 75.3% of the control beams' capacity with M5 (90% SL + 10% MK) and M6 (80% SL + 20% MK), respectively. The greatest capacity restoration was reached with the GP mix composed of 70% SL, 20% MK, and 10% SF, which resulted in an ultimate capacity of 2.99 kN—87.9% of the ultimate capacity of the control beams.

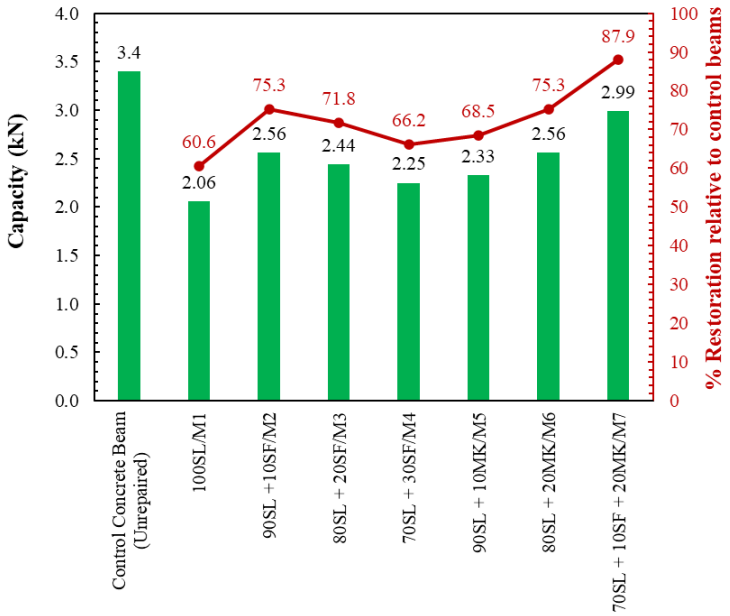
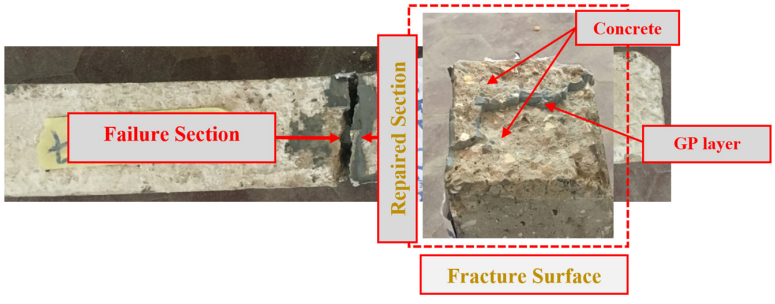
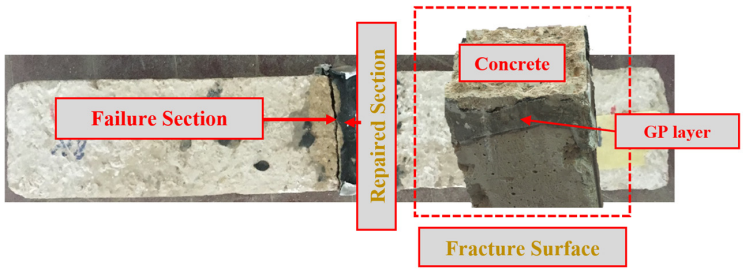


Figure 4. Flexural test results of the control and repaired beams.

Table 3 displays the failure modes for all repaired beams, while Figure 5 depicts the typical failure mode observed among the tested beams. As can be seen, the failure surface either developed solely within the concrete or passed through both the concrete and the GP layer, but without signs of complete debonding. This indicates strong adhesion between the GP layer and the concrete. Although in some beams, failure occurred in the concrete slightly away from the repaired section, they did not fully restore the capacity of the control beams. This could be attributed to the fact that, prior to repair, the beams were pre-loaded up to failure, which most likely developed micro-cracks at the concrete beam itself, especially around the fracture zone, which may lead to early failure in the second loading cycle after repair.



Failure in concrete and GP layer



Failure in concrete

Figure 5. Typical failure patterns of tested beams.

3.5. Using GP for Repairing Granite and Limestone

Figure 6 and Table 3 present the ultimate capacity of all tested granite and limestone blocks bonded by GP layers. With the SL mix (M1), the granite and limestone specimens could carry a load of up to 7.6 kN and 8.2 kN, respectively. When SF was blended with SL, a stronger bond between the blocks was achieved. For mixes with SL replaced by 10%, 20%, and 30% SF (M2-M4), the ultimate load carried by the bonded granite specimens increased by 23.7%, 21.1%, and 13.2%, respectively, compared to those bonded with the SL mix (M1). These increases reached up to 29.3%, 24.4%, and 28%, respectively, in the limestone specimens. Replacing SL with MK also enhanced the adhesion of GP to granite and limestone blocks. At replacement levels of 10% and 20% MK (M5–M6), the bonded granite specimens sustained an ultimate load of 7.9% and 21.1% higher than those sustained by specimens bonded with SL mix (M1). The improvements in the limestone specimens were 13.4% and 22% when M5 (90% SL + 10% MK) and M6 (80% SL + 20% MK), respectively, were used. The highest capacity was achieved in both granite and limestone specimens when the GP mix consisting of 70% SL + 20% MK + 10% SF was used, achieving a capacity of approximately 34% (in both block types) higher than those bonded with the SL mix (M1). The results also indicated that for the same GP mix, the bonded limestone specimens carried a relatively higher load than that carried by the bonded granite specimens. This could be attributed to the porous surface of the limestone, which may have helped to form a higher bonding with the GP layer, compared to the granite blocks that had a smoother surface with low porosity.

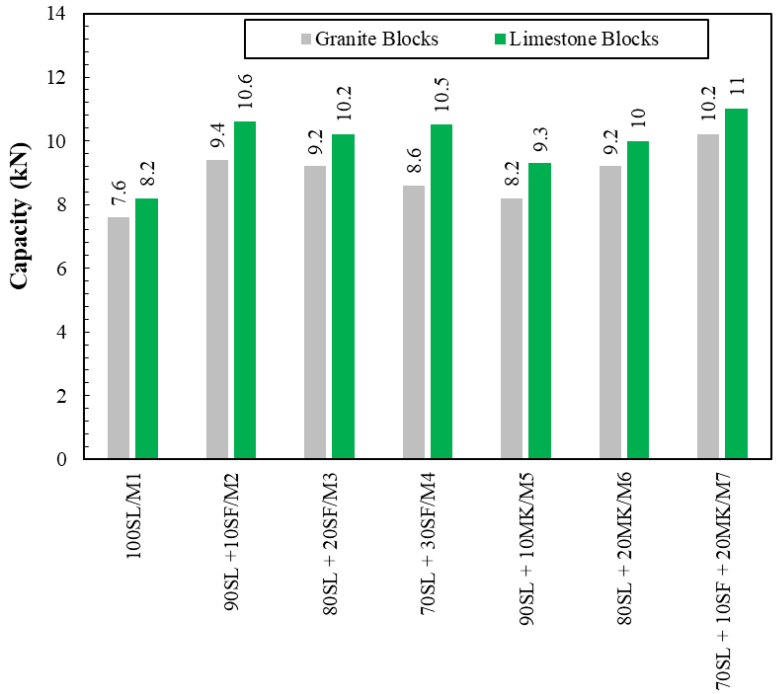


Figure 6. Flexural test results of the granite and limestone specimens.

By investigating the failure pattern, it was observed that in the granite specimens, the failure typically occurred at the interface (see Table 3 and Figure 7), which was the weakest zone relative to the high strength of both the granite and the GP layer. On the other hand, since the bonding between the limestone and GP layer was stronger, failure was not governed by interface debonding. Instead, different failure modes were observed, including failure in both the GP layer and the block, failure within the block, and failure that passed through both the block and the interface, as shown in Figure 7. The failure types experienced by each specimen are presented in Table 3.

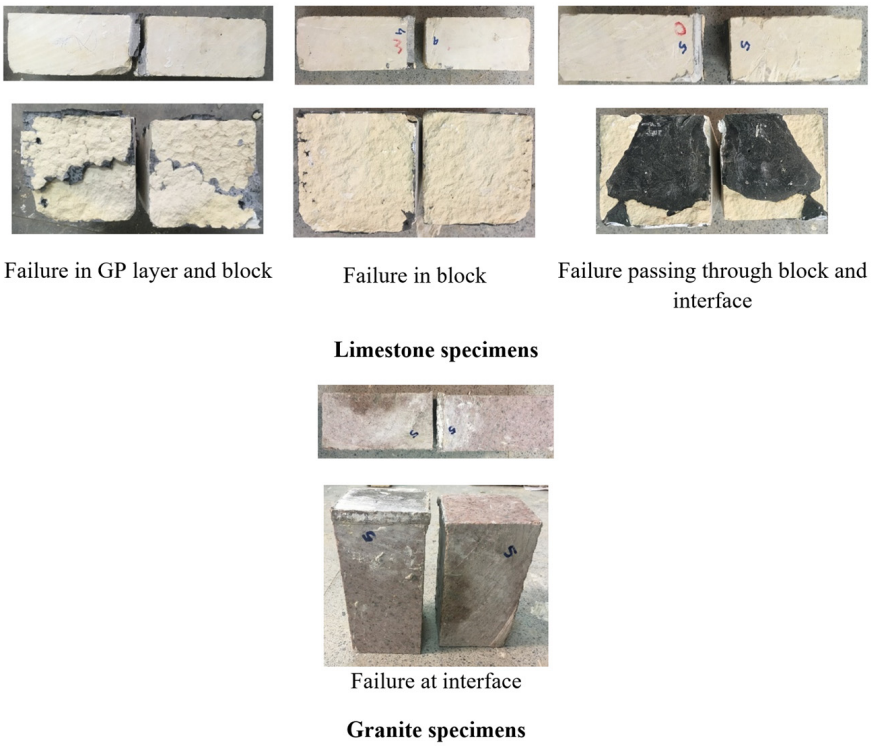


Figure 7. Typical failure patterns of tested limestone and granite specimens.

3.6. Evaluation of the Developed GPs Compared to a Commercial Epoxy Adhesive Mortar (EAM)

As per the test results obtained in this study, the developed GP mixes appeared to have a promising potential for being used as an adhesive agent in different applications, particularly in installing steel bars into hardened concrete and repairing either concrete or masonry structures. However, in order to evaluate the feasibility of the developed GPs for practical use, it was important to assess their performance compared to commercial adhesive agents in terms of mechanical properties and costs. For comparison, the M7 (70% SL + 20% MK + 10% SF) was selected since it had the highest mechanical and adhesive properties among the developed GP mixes. Looking at Table 4, it can be seen that in pull-out results, M7 had a bonding strength of 82.7% of that shown by the EAM. In repaired concrete beams, the capacity restored by M7 was around 90.6% of that restored by the EAM. For granite and limestone blocks bonded with M7, the load-carrying capacities were 87.9% and 91.7%, respectively, compared to the blocks bonded with the EAM. It is worth noting that M7 achieved this performance, despite its significantly low compressive strength and STS compared to the EAM (i.e., the EAM had a compressive strength and STS of 1.49 and 2.46 times as much as those of M7). To account for differences in compressive strength, all strength values were calculated and normalized by dividing by the square root of each material's compressive strength. Table 4 shows that the normalized values reflect comparable adhesive performance for both M7 and the EAM. This implies that, at comparable compressive strengths, the GP is likely provide superior adhesive performance compared to the EAM.

Table 4 also presents the estimated unit costs for both M7 and EAM. It is evident that M7 has a significantly lower cost, being produced at approximately 25% of the cost of EAM. This highlights the potential for developing a high-performance, cost-effective adhesive agent using geopolymers. Furthermore, the GP mix is environmentally friendly as it is a free-cement product made using industrial by-products such as SL and SF. This helps reduce carbon emissions associated with cement production and conserves natural resources. By leveraging such materials, the construction industry can move towards more sustainable practices while maintaining performance and functionality.

Table 4. Comparison between M7 (best GP mix) and commercial EAM.

	M7		EAM	
	Absolute Values	**Normalized Values**	**Absolute Values**	**Normalized Values**
Compressive strength (MPa)	47.7	-	71	-
STS (MPa)	2.85	-	7	-
Pull-out strength (MPa)	9.1	1.32	11	1.31
Concrete beams (MPa)	2.69	0.39	2.97	0.35
Granite blocks (MPa)	3.06	0.44	3.48	0.41
Limestone blocks (MPa)	3.30	0.48	3.60	0.43
Unit cost	1	-	3.9	-

4. Conclusions

This study investigated the mechanical and adhesive performance of different geopolymer paste (GP) mixes developed with a unary, binary and ternary binder system. The mechanical properties of the developed GPs and their adhesion to steel, concrete and granite/limestone were tested. A commercial epoxy adhesive mortar (EAM) was included for comparison. From the results described in this paper, the following conclusions can be drawn:

1. Using binder materials with high pozzolanic reactivity such as SF significantly improved the mechanical and adhesive properties of SL-based GP paste. The SF showed the optimal effect at a replacement level of 10%, while higher SF contents (20% and 30%) did not show further improvements.
2. Similar to SF, MK had a positive impact on improving the mechanical and adhesive properties of the SL-based GP paste. However, it was not possible to use replacements higher than 20% due to the workability restrictions.
3. Among the developed GP mixes, the combination of 70% SL, 20% MK and 10% SF showed the highest adhesive properties, which proved the high potential of using geopolymers as a bonding agent, even when it was compared to a higher compressive strength EAM.
4. In pull-out tests, using GP mixes improved the bonding between rebar and the concrete substrate by 19.7% to 49.2% compared to pre-installed rebar (i.e., rebar embedded in freshly poured concrete during casting).
5. Using GP mixes in the repair of concrete beams restored approximately 60.6% to 87.9% of the original load-carrying capacity of the control specimens.
6. The results for both granite and limestone indicate that GPs are a promising candidate for repair applications in masonry structures, often found in historic buildings. However, all GP mixes exhibited better bond strength with limestone than with granite, due to the porous texture of the limestone surface.
7. Compared to the commercial EAM investigated in this study, cost estimates indicate that using SL, SF, and MK allows for the development of a novel, eco-friendly, and cost-effective adhesive agent—approximately 25% of the cost of EAM—suitable for various applications in the construction industry.

Author Contributions: Conceptualization, T.Z.B., M.K.I., M.I.S. and A.M.R.; Methodology, T.Z.B., M.K.I., M.I.S. and A.M.R.; Validation, T.Z.B., M.K.I., M.I.S. and A.M.R.; Formal analysis, T.Z.B. and M.K.I.; Investigation, T.Z.B. and M.K.I.; Data curation, T.Z.B. and M.K.I.; Writing—original draft, T.Z.B.; Writing—review & editing, T.Z.B., M.K.I., M.I.S. and A.M.R.; Visualization, T.Z.B. and M.K.I.; Supervision, M.K.I., M.I.S. and A.M.R. All authors have read and agreed to the published version of the manuscript.

Funding: This research was facilitated with funding provided by the Faculty of Engineering, Cairo University, Giza, Egypt.

Data Availability Statement: The original contributions presented in the study are included in the article, further inquiries can be directed to the corresponding author.

Conflicts of Interest: The authors declare no conflict of interest.

References

1. Kim, J.H.J.; Lim, Y.M.; Won, J.P.; Park, H.G.; Lee, K.M. Shear capacity and failure behavior of DFRCC repaired RC beams at tensile region. *Eng. Struct.* **2007**, *29*, 121–131. [CrossRef]
2. Murthya, A.R.; Karihaloob, B.L.; Ranic, P.V.; Priyad, D.S. Fatigue Behaviour of Damaged RC Beams Strengthened with Ultra-High Performance Fibre Reinforced Concrete. *Int. J. Fatigue* **2018**, *116*, 659–668. [CrossRef]
3. Deng, M.; Ma, F.; Ye, W.; Li, F. Flexural Behavior of Reinforced Concrete Beams Strengthened by HDC and RPC. *Constr. Build. Mater.* **2018**, *188*, 995–1006. [CrossRef]
4. Zanotti, C.; Borges, P.H.R.; Bhutta, A.; Banthia, N. Bond Strength Between Concrete Substrate and Metakaolin Geopolymer Repair Mortar: Effect of Curing Regime and PVA Fiber Reinforcement. *Cem. Concr. Compos.* **2017**, *80*, 307–316. [CrossRef]
5. Khuram, R.; Ahmad, M.; Ueda, T.; Deng, J.; Aslam, K.; Nazir, I.; Azam, S.M. Experimental Investigation of the Bond Strength Between New to Old Concrete Using Different Adhesive Layers. *Constr. Build. Mater.* **2020**, *249*, 118798.
6. Momayez, A.; Ehsani, M.; Ramezanianpour, A.; Rajaie, H. Comparison of Methods for Evaluating Bond Strength Between Concrete Substrate and Repair Materials. *Cem. Concr. Res.* **2005**, *35*, 748–757. [CrossRef]
7. Zhang, D.; Ueda, T.; Furuuchi, H. Fracture Mechanisms of Polymer Cement Mortar: Concrete Interfaces. *J. Eng. Mech.* **2013**, *139*, 167–176. [CrossRef]
8. Mohammadi, M.; Moghtadaei, R.M.; Samani, N.A. Influence of Silica Fume and Metakaolin with Two Different Types of Interfacial Adhesives on the Bond Strength of Repaired Concrete. *Constr. Build. Mater.* **2014**, *51*, 141–150. [CrossRef]
9. Songpiriyakij, S.; Pulngern, T.; Pungpremtrakul, P.; Jaturapitakkul, C. Anchorage of Steel Bars in Concrete by Geopolymer Paste. *Mater. Des.* **2011**, *32*, 3021–3028. [CrossRef]
10. Phoo-ngernkham, T.; Chindaprasirt, P.; Sata, V.; Hanjitsuwan, S.; Hatanaka, S. The Effect of Adding Nano-Sio_2 and Nano-Al_2O_3 on Properties of High Calcium Fly Ash Geopolymer Cured at Ambient Temperature. *Mater. Des.* **2014**, *55*, 58–65. [CrossRef]
11. Phoo-ngernkham, T.; Maegawa, A.; Mishima, N.; Hatanaka, S.; Chindaprasirt, P. Effects of sodium hydroxide and sodium silicate solutions on compressive and shear bond strengths of FA-GBFS geopolymer. *Constr. Build. Mater.* **2015**, *91*, 1–8. [CrossRef]
12. Gomaa, E.; Gheni, A.A.; Kashosi, C.; ElGawady, M.A. Bond Strength of Eco-Friendly Class C Fly Ash-Based Thermally Cured Alkali-Activated Concrete to Portland Cement Concrete. *J. Clean. Prod.* **2019**, *235*, 404–416. [CrossRef]
13. Gomaa, E.; Gheni, A.A.; Kashosi, C.; ElGawady, M.A. Repair of Ordinary Portland Cement Concrete Using Ambient-Cured Alkaliactivated Concrete: Interfacial Behavior. *Cem. Concr. Res.* **2020**, *129*, 105968. [CrossRef]
14. Deja, J.; Uliasz-Bochenczyk, A.; Mokrzycki, E. CO_2 Emissions from Polish Cement Industry. *Int. J. Greenh. Gas Control* **2010**, *4*, 583–588. [CrossRef]
15. Ali, M.B.; Saidur, R.; Hossain, M.S. A review on emission analysis in cement industries. *Renew. Sustain. Energy Rev.* **2011**, *15*, 2252–2261. [CrossRef]
16. Zhao, X.; Liu, C.; Zuo, L.; Wang, L.; Zhu, Q.; Liu, Y.; Zhou, B. Synthesis and characterization of fly ash geopolymer paste for goaf backfill: Reuse of soda residue. *J. Clean. Prod.* **2020**, *260*, 121045. [CrossRef]
17. Saha, S.; Rajasekaran, C. Enhancement of the Properties of Fly Ash Based Geopolymer Paste by Incorporating Ground Granulated Blast Furnace Slag. *Constr. Build. Mater.* **2017**, *146*, 615–620. [CrossRef]
18. Duxson, P.; Provis, J.L.; Lukey, G.C.; van Deventer, J.S. The Role of Inorganic Polymer Technology in the Development of 'Green Concrete'. *Cem. Concr. Res.* **2007**, *37*, 1590–1597. [CrossRef]
19. Bentz, D.P.; De la Varga, I.; Muñoz, J.F.; Spragg, R.P.; Graybeal, B.A.; Hussey, D.S.; Jacobson, D.L.; Jones, S.Z.; LaManna, J.M. Influence of Substrate Moisture State and Roughness on Interface Microstructure and Bond Strength: Slant Shear vs. Pull-Off Testing. *Cem. Concr. Compos.* **2018**, *87*, 63–72. [CrossRef]
20. Beushausen, H.; Höhlig, B.; Talotti, M. The Influence of Substrate Moisture Preparation on Bond Strength of Concrete Overlays and the Microstructure of the OTZ. *Cem. Concr. Res.* **2017**, *92*, 84–91. [CrossRef]
21. Wang, Y.S.; Peng, K.D.; Alrefaei, Y.; Dai, J.G. The bond between geopolymer repair mortars and OPC concrete substrate: Strength and microscopic interactions. *Cem. Concr. Compos.* **2021**, *119*, 103991.
22. Ariyadasa, P.W.; Manalo, A.C.; Lokuge, W.; Aravinthan, V.; Pasupathy, K.; Gerdes, A. Bond performance of fly ash-based geopolymer mortar in simulated concrete sewer substrate. *Constr. Build. Mater.* **2024**, *446*, 137927. [CrossRef]
23. Albidah, A.; Abadel, A.; Alrshoudi, F.; Altheeb, A.; Abbas, H.; Al-Salloum, Y. Bond strength between concrete substrate and metakaolin geopolymer repair mortars at ambient and elevated temperatures. *J. Mater. Res. Technol.* **2020**, *9*, 10732–10745. [CrossRef]
24. Ding, Y.C.; Cheng, T.W.; Dai, Y.S. Application of geopolymer paste for concrete repair. *Struct. Concr.* **2017**, *18*, 561–570. [CrossRef]
25. Ahmad Zailani, W.W.; Bouaissi, A.; Abdullah, M.M.A.B.; Abd Razak, R.; Yoriya, S.; Mohd Salleh, M.A.A.; Rozainy MAZ, M.R.; Fansuri, H. Bonding strength characteristics of FA-based geopolymer paste as a repair material when applied on OPC substrate. *Appl. Sci.* **2020**, *10*, 3321. [CrossRef]
26. Frangieh, C.; Saba, M.; Karmaoui, D.; Lafhaj, Z. Geopolymer: A new sustainable repairing material for concrete cracks. In *IOP Conference Series: Earth and Environmental Science*; IOP Publishing: Bristol, UK, 2022; Volume 1123, p. 012061.

27. Chen, K.; Wu, D.; Yi, M.; Cai, Q.; Zhang, Z. Mechanical and durability properties of metakaolin blended with slag geopolymer mortars used for pavement repair. *Constr. Build. Mater.* **2021**, *281*, 122566. [CrossRef]
28. Maras, M.M. Characterization of performable geopolymer mortars for use as repair material. *Struct. Concr.* **2021**, *22*, 3173–3188. [CrossRef]
29. Hai, R.; Zheng, J.; Li, J.; Hui, C.; Liu, J. Preparation mechanism and properties of thermal activated red mud and its geopolymer repair mortar. *Case Stud. Constr. Mater.* **2024**, *20*, e02853. [CrossRef]
30. Zheng, C.; Mao, Z.; Chen, L.; Qian, H.; Wang, J. Development of a novel rapid repairing agent for concrete based on GFRP waste powder/GGBS geopolymer mortars. *J. Build. Eng.* **2023**, *71*, 106542. [CrossRef]
31. *ASTM C989/C989M*; Standard Specification for Slag Cement for Use in Concrete and Mortars. ASTM International: West Conshohocken, PA, USA, 2022.
32. *ASTM C1240*; Standard Specification for Silica Fume Used in Cementitious Mixtures. ASTM International: West Conshohocken, PA, USA, 2020.
33. *ASTM C618*; Standard Specification for Coal Fly Ash and Raw or Calcined Natural Pozzolan for Use in Concrete. ASTM International: West Conshohocken, PA, USA, 2023.
34. *ASTM C494/C494M-13*; Standard Specification for Chemical Admixtures for Concrete. ASTM International: West Conshohocken, PA, USA, 2020.
35. *ASTM C881/C881M*; Standard Specification for Epoxy-Resin-Base Bonding Systems for Concrete. ASTM International: West Conshohocken, PA, USA, 2020.
36. *ASTM C150/C150M*; Standard Specification for Portland Cement. ASTM International: West Conshohocken, PA, USA, 2012.
37. Hadi, M.N.S.; Farhan, N.A.; Sheikh, M.N. Design of Geopolymer Concrete with GGBFS At Ambient Curing Condition Using Taguchi Method. *Constr. Build. Mater.* **2017**, *140*, 424–431. [CrossRef]
38. Mohseni, E. Assessment of Na_2SiO_3 to NaOH Ratio Impact on the Performance of Polypropylene Fiber-Reinforced Geopolymer Composites. *Constr. Build. Mater.* **2018**, *186*, 904–911. [CrossRef]
39. EFNARC. *The European Guidelines for Self-Compacting Concrete Specification, Production and Use*, English ed.; European Federation for Specialist Construction Chemicals and Concrete Systems: Norfolk, UK, 2005.
40. *ASTM C109/C109M*; Standard Test Method for Compressive Strength of Hydraulic Cement Mortars (Using 2-in. or [50-mm] Cube Specimens). ASTM International: West Conshohocken, PA, USA, 2020.
41. Jindal, B.B. Investigations on the properties of geopolymer mortar and concrete with mineral admixtures: A review. *Constr. Build. Mater.* **2019**, *227*, 116644. [CrossRef]
42. Ismail, M.K.; Hassan, A.A.A.; Lachemi, M. Abrasion Resistance of Self-Consolidating Engineered Cementitious Composites Developed with Different Mixture Compositions. *ACI Mater. J.* **2019**, *116*, 27–38.
43. Hassan, A.A.A.; Lachemi, M.; Hossain, K.M.A. Effect of Metakaolin and Silica Fume on Rheology of Self-Consolidating Concrete. *ACI Mater. J.* **2012**, *109*, 657–664.
44. Alanazi, H.; Hu, J.; Kim, Y.R. Effect of slag, silica fume, and metakaolin on properties and performance of alkali-activated fly ash cured at ambient temperature. *Constr. Build. Mater.* **2019**, *197*, 747–756.
45. Okoye, F.N.; Prakash, S.; Singh, N.B. Durability of Fly Ash Based Geopolymer Concrete in the Presence of Silica Fume. *J. Clean. Prod.* **2017**, *149*, 1062–1067. [CrossRef]
46. Görhan, G.; Aslaner, R.; Şinik, O. The effect of curing on the properties of metakaolin and fly ash-based geopolymer paste. *Compos. Part B Eng.* **2016**, *97*, 329–335. [CrossRef]
47. Cheah, C.B.; Tan, L.E.; Ramli, M. The Engineering Properties and Microstructure of Sodium Carbonate Activated Fly Ash/Slag Blended Mortars with Silica Fume. *Compos. Part B Eng.* **2019**, *160*, 558–572. [CrossRef]

Disclaimer/Publisher's Note: The statements, opinions and data contained in all publications are solely those of the individual author(s) and contributor(s) and not of MDPI and/or the editor(s). MDPI and/or the editor(s) disclaim responsibility for any injury to people or property resulting from any ideas, methods, instructions or products referred to in the content.